Annals of Nuclear Medicine (2022) 36:310–318
https://doi.org/10.1007/s12149-021-01705-5

ORIGINAL ARTICLE

Dual time point imaging of staging PSMA PET/CT quantification; spread and radiomic analyses

Ayşegül Aksu[1] · Özge Vural Topuz[1] · Gülşah Yılmaz[1] · Gamze Çapa Kaya[2] · Burçak Yılmaz[1]

Received: 3 October 2021 / Accepted: 29 November 2021 / Published online: 6 January 2022

Abstract

Objective The aims were to evaluate the performance of models that predict Gleason Grade (GG) groups with radiomic data obtained from the prostate gland in dual time 68Ga-Prostate Specific Membrane Antigen (PSMA) Positron Emission Tomography/Computerized Tomography (PET/CT) images for prostate cancer (PCa) staging, and to analyze the contribution of late imaging to the radiomic model and to evaluate the relationship of the distance between tumor foci in the body (Dmax) obtained in early PET images with histopathology and prostate specific antigen (PSA) value.

Methods Between October 2020 and August 2021, 41 patients who underwent 68Ga-PSMA PET/CT for staging of PCa were retrospectively analyzed. Volumetric and radiomics data were obtained from early and late PSMA PET images. The differences between age, metastasis status, PSA, standard uptake value (SUV), volumetric and radiomics parameters between GG groups were analyzed. Early and late PET radiomic models were created, area under curve (AUC), sensitivity, specificity and accuracy values of the models were obtained. In addition, the correlation of Dmax values with total PSMA-tumor volume (TV), Total lesion (TL)-PSMA and PSA values was evaluated. In metastatic patients, the difference in Dmax between GG groups was analyzed.

Results There was a significant difference between patients with GG ≤ 3 and > 3 in 35 of the early PET radiomic features. In the early PET model, multivariate analyses showed that GLRLM_RLNU and PSA were the most meaningful parameters. The AUC, sensitivity, specificity and accuracy values of the early model in detecting patients with GG > 3 were calculated as 0.902, 76.2%, 84% and 78.1%, respectively. In 36 late PET radiomic features, there was a significant difference between patients with GG ≤ 3 and > 3. In multivariate analyses; SHAPE_compacity and PSA were obtained as the most meaningful parameters. The AUC, sensitivity, specificity and accuracy values of the late model in detecting patients with GG > 3 were calculated as 0.924, 85.7%, 85% and 85.4%. There was a strong correlation between Dmax and PSA values ($p < 0.001$, rho: 0.793). Dmax showed strong correlation with PSMA-TVtotal and TL-PSMAtotal ($p < 0.001$, rho: 0.797; $p < 0.001$, rho: 0.763, respectively). In patients with metastasis, median Dmax values of the GG > 3 group were higher than GG ≤ 3 group; A statistically significant difference was obtained between these two groups ($p = 0.023$).

Conclusions Model generated from the late PSMA PET radiomic data had better performance in the current study. Without the use of invasive methods, the heterogeneity and aggressiveness of the primary tumor and the prediction of GG groups may be possible with 68Ga-PSMA PET/CT images obtained for diagnostic purposes especially with late PSMA PET/CT imaging.

Keywords Dual time point imaging · PSMA · PET · Radiomic · Dmax

Introduction

Prostate-specific membrane antigen (PSMA) is a molecular target of interest in both clinical imaging and radionuclide treatment of prostate cancer (PCa) [1–3]. Positron Emission Tomography (PET)/computerized tomography (CT) imaging using 68Ga-PSMA ligands is a highly sensitive method for detecting primary tumor as well as local recurrence and/or metastatic lesions after primary PCa treatment [4]. In

✉ Ayşegül Aksu
aaysegulgedikli@gmail.com

[1] Department of Nuclear Medicine, Başakşehir Cam and Sakura City Hospital, Istanbul, Turkey

[2] Department of Nuclear Medicine, School of Medicine, Dokuz Eylul University, Izmir, Turkey

addition to maximum standardized uptake value (SUVmax), the use of volumetric parameters in the evaluation of PSMA PET has also been investigated, and it has been reported that volumetric parameters can be used in both staging and treatment response [5–7]. Moreover, an imaging feature called the "distance between the two most distant lesions (Dmax)", which reflects the spread of the disease, has recently entered the literature, but its role in prostate cancer staging has not yet been investigated [8].

Radiomic is a rapidly developing field of research that expresses the acquisition and analyses of quantitative data from medical imaging with mathematical methods [9]. Recently, interest in the radiomics approach has increased and there are studies suggesting that radiomics may help in the diagnosis, prognosis and treatment response of the diseases [10–13]. There are also very recently published reports with radiomic analyses for PSMA PET in PCa which examined the success of PSMA-PET radiomics in distinguishing Gleason Grade (GG) groups [14–16].

When dual time-point 68Ga-PSMA PET/CT imaging was evaluated, it was shown that there was a significant increase in SUVmax of PCa lesions in delayed images compared to early images [17, 18]. However, to our knowledge, there is no study on radiomic analyses from late PSMA PET images yet.

Combining all these data, we set two aims for our study. Our first aim was to evaluate the performance of models that predict GG groups with radiomic data obtained from the prostate gland in early and late 68Ga-PSMA PET/CT images, and to analyze the contribution of late imaging to the radiomic model. Our second aim was to evaluate the relationship of Dmax obtained in early PET images with histopathology and PSA value, and to analyze the place of this quantitative parameter in staging 68Ga-PSMA PET/CT.

Materials and methods

Patient group

Patients who underwent 68Ga-PSMA Imaging & Therapy (I&T) PET/CT for staging of PCa between October 2020 and August 2021 in our institution were evaluated retrospectively. Thirteen patients with PSMA uptake below 64 voxels in the prostate gland were excluded from the study (because VOI below 64 voxels cannot technically be evaluated with Local Images Features extraction-LIFEx software) [19]. A total of 41 male patients with a diagnosis of prostate adenocarcinoma who had no history of PCa specific treatment and had not undergone prostatectomy were included in the study.

Grade groups obtained from 12-quadrant biopsy material were used. GG groups were determined according to the Gleason Grading system suggested by the International Society of Urological Pathology (ISUP) in 2014 [20]. According to their GG, the patients were divided into two groups as $GG \leq 3$ and $GG > 3$.

68Ga-PSMA PET/CT ımaging

All patients were informed both orally and written for PET/CT imaging. 68Ga-PSMA I&T was synthesized with Scintomics (Germany) full automatic synthesis unit. After production, labeling efficacy was assessed with high-performance liquid chromatography. Mean 5.0 millicurie (mCi) (185 Megabecquerel-MBq) 68Ga-PSMA I&T injection was performed. Approximately 45 ± 5 min after injection, low-dose CT was used for attenuation correction with the following parameters: 113 mAS, 120 kV and 4 mm section thickness. Following CT images, early PET images were obtained for 1.5 min in each bed position in supine position from vertex to mid-thigh with Philips Ingenuity TF 64 PET/CT (Philips Medical Systems, Cleveland OH, USA). After an average of 45 min from the first imaging, late PET images were obtained in the pelvic region for 1.5 min in two bed positions just after micturation. All patients had both early and late 68Ga-PSMA PET/CT images. Images were reconstructed using iterative ordered subset expectation maximization reconstruction with 3 iterations and 33 subsets, and with 4-mm voxel dimensions.

Volumetric analyses

Visual evaluation was performed by two experienced nuclear medicine physicians (AA and BY). According to PSMA-RADs criteria, lesions in categories 4 and 5 were considered metastatic in early 68Ga-PSMA PET/CT images [21]. Areas with PSMA uptake were anatomically localized with non-diagnostic CT images. In the LIFEx software, there is a separate section -MTV protocol- where volumetric analyses are performed, along with the area where the texture features are extracted [19, 22]. PSMA uptakes over 2.5 SUVmax in the whole body were detected semiautomatically with the MTV protocol of the LIFEx software. Later, the physiological activities demonstrating a SUV greater than 2.5 were deleted manually one by one. Tumor volume (PSMA-TV) and SUVmean values were obtained from all volumes of interest (VOI) in early PET/CT images. Total lesion PSMA (TL-PSMA) values were calculated by multiplying SUVmean and PSMA-TV. Whole body tumor volume (PSMA-TVtotal) and tumor burden (TL-PSMAtotal) values were obtained by summing all PSMA-TV and TL-PSMA values from the VOIs associated with PCa. Dmax values were obtained in the MTV protocol; the distances between all obtained VOIs were automatically calculated by LIFEx software using the Euclidean distance between their centers [8, 19] (Fig. 1). The highest value among all counted values

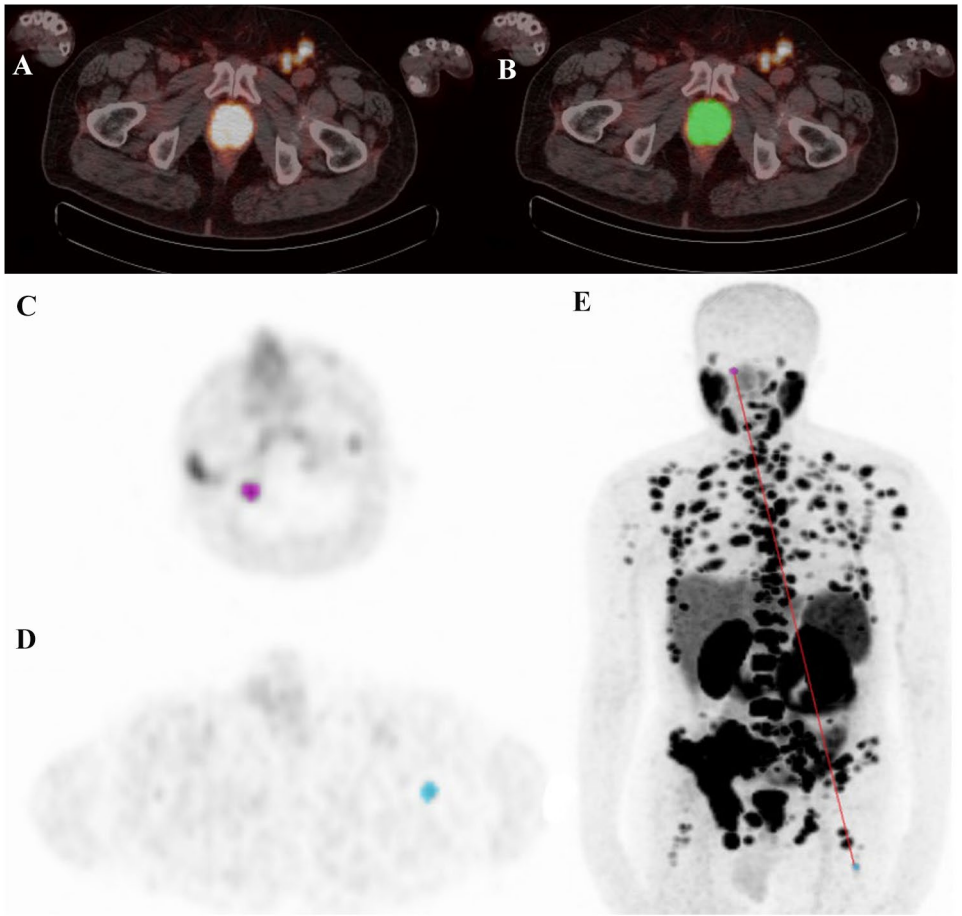

Fig. 1 68Ga-PSMA PET image process. **A** and **B** show segmentation of PSMA uptake in the prostate gland. **A** 68Ga-PSMA PET/CT fusion images and **B** the segmented area (with green color). **C**, **D**, and **E** visualize the determination of the furthest distance between two tumor foci. The red line shows the furthest distance between the VOI's that associated with metastatic foci and this quantitative value is calculated automatically by LIFEx software

was determined as Dmax. Dmax value was noted as zero in patients without metastasis.

Texture analyses

The feature extraction was performed by LIFEx software [22]. PSMA uptake above 2.5 SUV in the prostate gland was segmented in both early and late 68Ga-PSMA PET/CT images [22] (Fig. 1). Forty-one features were extracted from these segmented areas. Conventional parameters, shape parameters, second order-based (gray-level co-occurrence matrix—GLCM), and high order-based (neighborhood gray-level different matrix—NGLDM, gray-level run-length matrix—GLRLM, and gray-level zone-length matrix—GLZLM) features obtained from the analyses are presented in Table 1. Texture matrices were re-sampled at $4 \times 4 \times 4$ mm, with 64 fixed bin numbers and absolute scale bounds between 0 and 50.

Statistical analyses

The free version of the Statistical Package for the Social Sciences (SPSS) v. 28.0 was used for the statistical analyses. A p value of < 0.05 was considered significant. Normally distributed data were presented as mean ± standard deviation, and non-normal distributed data were given as median (range).

The correlation between PSMA-TVtotal, TL-PSMAtotal, Dmax and PSA values in all patients was evaluated by Spearman correlation analyses. The differences between age, PSA, SUV, volumetric and texture analyses parameters between GG groups were analyzed by the Mann–Whitney U test. The relationship between categorical variables was evaluated by chi-square or Fisher exact tests.

Spearman correlation analyses was used to evaluate the correlation between the features that were found to be significant in the GG groups. The features with a correlation coefficient of less than 0.8 were analyzed with logistic regression; the others were not included in the further analyses [23]. Two different models were created with early and late PET radiomic features. The model performance was evaluated by area under curve (AUC) obtained from the receiver operating characteristic analyses. The

Table 1 Extracted features by LIFEx software

Conventional	SUVmax, SUVmean, SUVstd, SUVpeak, TL-PSMA
Shape-based	PSMA-TV, sphericity, compacity, surface
GLCM	Homogeneity, energy, contrast, correlation, entropy (log 2&10), dissimilarity
GLRLM	SRE, LRE, LGRE, HGRE, SRLGE, SRHGE, LRLGE, LRHGE, GLNU, RLNU, RP
NGLDM	Coarseness, contrast, busyness
GLZLM	SZE, LZE, LGZE, HGZE, SLZLGE, SZHGE, LZLGE, LZHGE, GLNU, ZLNU, ZP

SUV standard uptake value, *TL-PSMA* total lesion PSMA, *PSMA-TV* PSMA tumor volume, *GLCM* gray-level co-occurrence matrix, *GLRLM* gray level run length matrix, *NGLDM* neighborhood gray-level different matrix, *GLZLM* gray level zone length matrix, *SRE* short-run emphasis, *LRE* long-run emphasis, *LGRE* low gray-level run emphasis, *HGRE* high gray-level run emphasis, *SRLGE* short-run low gray-level emphasis, *SRGHE* short-run high gray-level emphasis, *LRLGE* long-run low gray-level emphasis, *LRHGE*. long-run high gray-level emphasis, *GLNU* gray-level non-uniformity, *RLNU* run length non-uniformity, *RP* run percentage, *SZE* short-zone emphasis, *LZE* long-zone emphasis, *LGZE* low gray-level zone emphasis, *HGZE* high gray-level zone emphasis, *SZLGE* short-zone low gray-level emphasis, *SZHGE* short-zone high gray-level emphasis, *LZLGE* long-zone low gray-level emphasis, *LZHGE* long-zone high gray-level emphasis, *ZLNU* zone length non-uniformity, *ZP* zone percentage

Table 2 The number of patients in Gleason Grade groups, D'Amico risk groups, the median (range) values of PSA, PSMA-TVtotal, TL-PSMAtotal and Dmax

Age (year)	69 ± 8 (53–85)
Gleason Grade 1 (*n*)	2 (4.9%)
Gleason Grade 2 (*n*)	13 (31.7%)
Gleason Grade 3 (*n*)	5 (12.2%)
Gleason Grade 4 (*n*)	11 (26.8%)
Gleason Grade 5 (*n*)	10 (24.4%)
Without metastasis (*n*)	17 (41.5%)
With metastasis (*n*)	24 (58.5%)
D'Amico medium risk (*n*)	7 (17.1%)
D'Amico high risk (*n*)	34 (82.9%)
PSA (ng/ml)	21.0 (4.0–1350.0)
PSMA-TVtotal (ml)	36.5 (4.8–5161.2)
TL-PSMAtotal (g)	159.8 (16.6–33,844.3)
Dmax (cm)	9.2 (0.0–105.8)

sensitivity, specificity and accuracy values of the models were calculated.

Ethical approval

Local ethics committee approval was obtained. All procedures performed in studies involving human participants were in accordance with the ethical standards of the institutional research committee and with the 1964 Helsinki declaration and its later amendments or comparable ethical standards.

Results

The mean age of the patients was 69 ± 8 years (range 53–85 years). General information about the patients is presented in Table 2.

The median PSA value of patients without metastasis was 11.8 ng/dl (4.3–96.0), and of patients with metastasis was 56.2 ng/dl (8.9–1350.0) and there was statistically significant difference between two groups ($p < 0.001$).

The median PSA value of patients with GG ≤ 3 was 14.2 ng/dl (4.3–99.2), and of patients with GG > 3 was 63.0 ng/dl (7.4–1350.0) ($p < 0.001$). The rate of metastasis was 30% in patients with GG ≤ 3 and 85.7% in patients with GG > 3 ($p < 0.001$).

Volumetric results

There was a strong correlation between Dmax and PSA values ($p < 0.001$, rho: 0.793). Dmax showed strong correlation with PSMA-TVtotal and TL-PSMAtotal ($p < 0.001$, rho: 0.797; $p < 0.001$, rho: 0.763, respectively). While Dmax was moderately correlated with prostate SUVmax and PSMA-TVprostate ($p = 0.001$, rho: 0.426; $p < 0.001$, rho: 0.593, respectively), TL-PSMA prostate was strongly correlated with Dmax ($p < 0.001$, rho: 0.613).

Median PSMA-TVtotal value was 17.3 ml (4.8–46.7) in the GG ≤ 3 group, and 200.4 ml (6.1–5161.2) in GG > 3 group, There was statistically significant difference between these groups ($p < 0.001$, AUC: 0.936, 0.854–1.000, 95% CI). GG > 3 group had higher TL-PSMA values (median 1653.2, range 20.0–33,844.3) than GG ≤ 3 group (median 65.7, range 16.6–270.4) ($p < 0.001$, AUC: 0.931, 0.841–1.000, 95% CI).

In patients with metastasis, median Dmax values of GG > 3 group were higher (median 39.7 cm, 8.6–105.8) than GG ≤ 3 group (median 9.4, range 5.4–31.3). A statistically significant difference was obtained between these two groups ($p = 0.023$, AUC: 0.815, 0.608–1.000, 95% CI).

Early PET radiomic analyses

There was a significant difference between patients with GG ≤ 3 and > 3 in 35 of the early PET radiomic features. The texture feature with the highest ability to differentiate these groups was GLRLM_RLNU ($p < 0.001$, AUC: 0.879, 0.776–0.991, 95% CI). The patients with GG > 3 had higher GLRLM_RLNU value than patients with GG ≤ 3. The early PET features with statistically significant differences between GG groups are shown in Table 3. The features with a correlation coefficient of less than 0.8 (Fig. 2), GLRLM_RLNU and GLCM_dissimilarity, were analyzed with a

Table 3 *p* values and AUC of the features with significant difference between GG ≤ 3 and > 3 patients

Features	Early PET imaging		Late PET imaging	
	p value	AUC (95% CI)	*p* value	AUC (95% CI)
SUVmean	0.001	0.800 (0.667–0.933)	< 0.001	0.842 (0.724–0.959)
SUVstd	0.003	0.768 (0.623–0.913)	0.003	0.770 (0.624–0.916)
SUVmax	0.007	0.745 (0.595–0.895)	0.002	0.780 (0.636–0.923)
SUVpeak	0.006	0.752 (0.604–0.901)	0.002	0.793 (0.654–0.933)
TL-PSMA	< 0.001	0.874 (0.760–0.987)	< 0.001	0.890 (0.787–0.994)
PSMA-TV	< 0.001	0.864 (0.752–0.976)	< 0.001	0.877 (0.767–0.988)
SHAPE_sphericity	0.404	NS	0.575	NS
SHAPE_surface	< 0.001	0.838 (0.716–0.960)	< 0.001	0.860 (0.739–0.980)
SHAPE_compacity	< 0.001	0.867 (0.750–0.983)	< 0.001	0.910 (0.820–1.000)
GLCM_homogeneity	0.010	0.735 (0.583–0.886)	0.006	0.751 (0.604–0.898)
GLCM_energy	< 0.001	0.830 (0.705–0.955)	< 0.001	0.854 (0.740–0.968)
GLCM_contrast	0.022	0.710 (0.548–0.871)	0.025	0.705 (0.542–0.868)
GLCM_correlation	0.001	0.804 (0.671–0.936)	< 0.001	0.864 (0.756–0.972)
GLCM_Entropy log 10	< 0.001	0.821 (0.695–0.948	< 0.001	0.845 (0.729–0.962)
GLCM_Entropy log 2	< 0.001	0.821 (0.695–0.948	< 0.001	0.845 (0.729–0.962)
GLCM_Dissimilarity	0.020	0.712 (0.554–0.869)	0.022	0.710 (0.548–0.871)
GLRLM_SRE	0.013	0.727 (0.573–0.882)	0.007	0.746 (0.598–0.895)
GLRLM_LRE	0.019	0.714 (0.557–0.872)	0.011	0.731 (0.578–0.884)
GLRLM_LGRE	< 0.001	0.830 (0.706–0.954)	< 0.001	0.879 (0.776–0.981)
GLRLM_HGRE	< 0.001	0.800 (0.667–0.933)	0.001	0.817 (0.688–0.945)
GLRLM_SRLGE	< 0.001	0.840 (0.721–0.960)	< 0.001	0.883 (0.783–0.984)
GLRLM_SRHGE	0.002	0.781 (0.642–0.920)	0.001	0.805 (0.671–0.938)
GLRLM_LRLGE	0.001	0.790 (0.653–0.928)	< 0.001	0.850 (0.736–0.964)
GLRLM_LRHGE	0.001	0.805 (0.672–0.936)	< 0.001	0.836 (0.714–0.958)
GLRLM_GLNU	0.220	NS	0.035	0.693 (0.529–0.857)
GLRLM_RLNU	< 0.001	0.879 (0.766–0.991)	< 0.001	0.890 (0.788–0.993)
GLRLM_RP	0.018	0.715 (0.558–0.873)	0.011	0.732 (0.580–0.884)
NGLDMcoarseness	0.001	0.796 (0.659–0.933)	< 0.001	0.844 (0.722–0.966)
NGLDMcontrast	0.175	NS	0.273	NS
NGLDMbusyness	0.211	NS	0.206	NS
GLZLM_SZE	0.016	0.720 (0.559–0.881)	0.011	0.731 (0.572–0.890)
GLZLM_LZE	0.045	0.683 (0.519–0.848)	0.045	0.683 (0.520–0.847)
GLZLM_LGZE	0.002	0.779 (0.639–0.919)	0.001	0.798 (0.664–0.931)
GLZLM_HGZE	0.004	0.764 (0.619–0.910)	0.003	0.774 (0.629–0.919)
GLZLM_SZLGE	0.667	NS	0.676	NS
GLZLM_SZHGE	0.006	0.750 (0.601–0.899)	0.005	0.757 (0.607–0.908)
GLZLM_LZLGE	0.011	0.733 (0.578–0.889)	0.009	0.738 (0.587–0.889)
GLZLM_LZHGE	0.958	NS	0.774	NS
GLZLM_GLNU	< 0.001	0.836 (0.704–0.967)	< 0.001	0.894 (0.790–0.998)
GLZLM_ZLNU	< 0.001	0.824 (0.697–0.951)	< 0.001	0.848 (0.733–0.962)
GLRLM_ZP	0.029	0.699 (0.539–0.859)	0.025	0.705 (0.544–0.866)

NS not significant

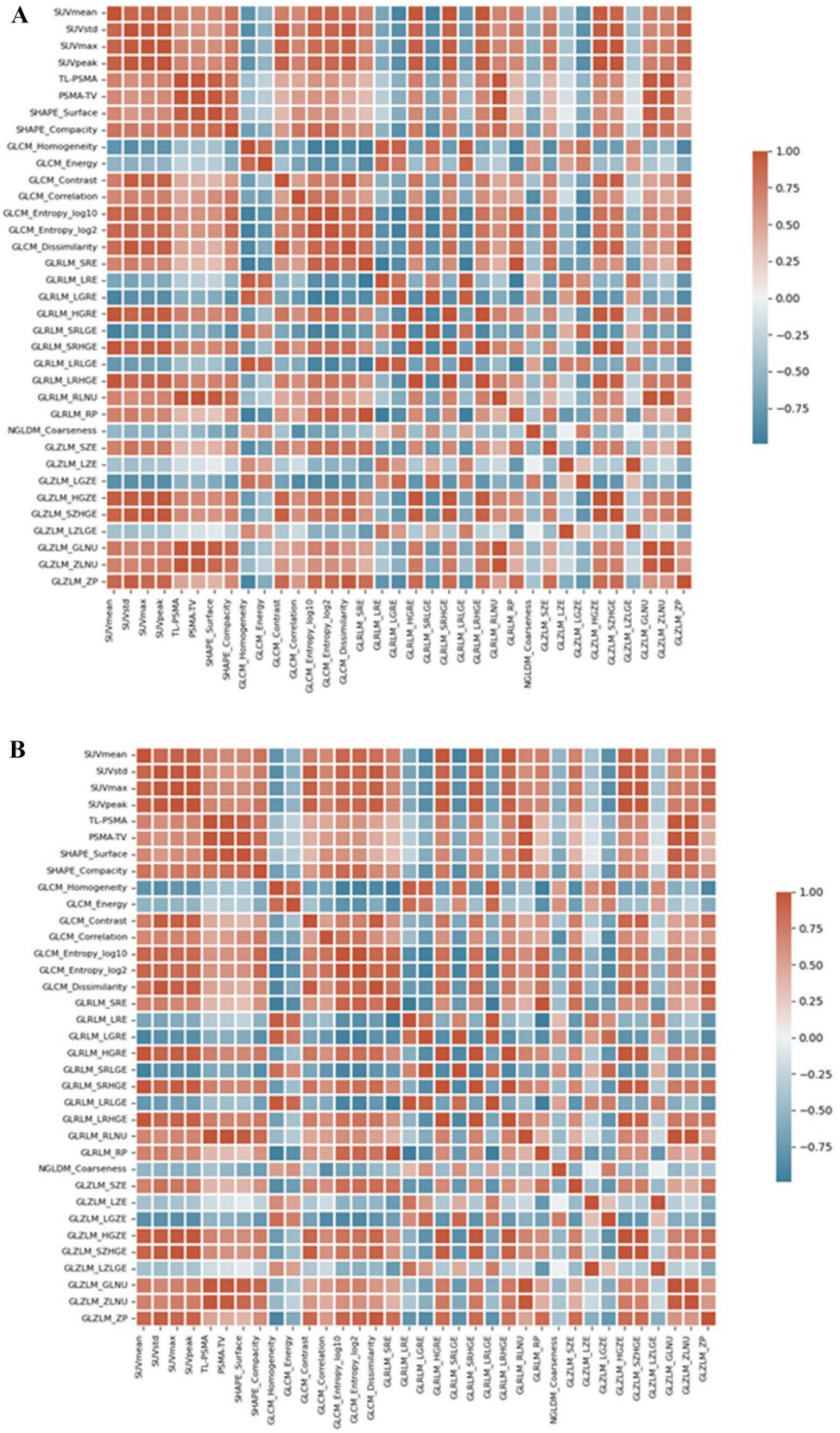

Fig. 2 Correlation matrix of significant features between Gleason Grade groups. Correlations were assessed using the Spearman correlation coefficient. In both *x* and *y* axes, the same features that showed significant differences between the GG groups were defined. The red color defines the positive correlation and the blue color defines the negative correlation. **A** Correlation matrix of early PET radiomic features. **B** Correlation matrix of late PET radiomic features

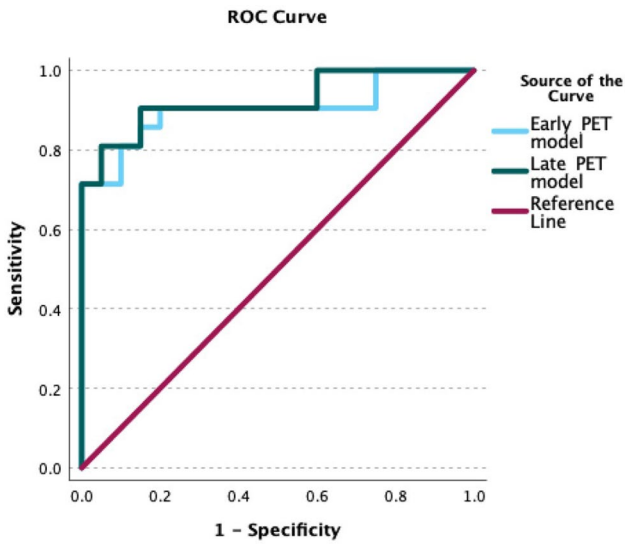

Fig. 3 ROC curves of the radiomic models (late model AUC: 0.924, early model AUC: 0.902)

Table 4 Formula of models obtained with logistic regression using radiomics data and PSA values

Early PET formula	(GLRLM_RLNU*0.005) + (PSA*0.029)-3.012
Late PET formula	(SHAPEcompacity*1.122) + (PSA*0.027)-6.191

GLRLM_RLNU gray level run length matrix-run length non-uniformity, *PSA* prostate specific antigen

logistic regression to build a model. In addition, age, PSA and metastasis status were added to the model. Multivariate analyses demonstrated that GLRLM_RLNU (p = 0.019, OR 1.006, 1.001–1.010, 95% CI) and PSA (p = 0.036, OR 1.030, 1.002–1.058, 95% CI) were the most meaningful parameters. Age and metastasis status could not be obtained as a significant prognostic factor in multivariate analyses. The early model's AUC was calculated as 0.902 (0.801–1.000, 95% CI, $p < 0.001$) (Fig. 3). The formula of the model is given in Table 4. The sensitivity, specificity and accuracy values of the model in detecting patients with GG > 3 were calculated as 76.2%, 84% and 78.1%, respectively.

Late PET radiomic analyses

There was a significant difference between patients with GG ≤ 3 and > 3 in 36 of the late PET radiomic features. The feature with the highest AUC value was SHAPE_compacity ($p < 0.001$, AUC: 0.910, 0.820–1.000, 95% CI). The patients with GG > 3 had higher SHAPE_compacity value than patients with GG ≤ 3. The other late PET features with statistically significant differences between GG groups are shown in Table 3. Among these features, the correlation between SHAPE_compacity, GLZLM_SZHGE and GLRLM_GLNU was less than 0.8 (Fig. 2). In multivariate analyses in which these features and age, PSA and metastasis status were included, only SHAPE_compacity (p = 0.008, OR 3.071, 1.339–7.040, 95% CI) and PSA (p = 0.049, OR 1.027, 1.001–1.056, 95% CI) were obtained as the most meaningful parameters. For the late model, age and metastasis status were not found to be significant prognostic factors in multivariate analyses either. The AUC value of the late model was determined as 0.924 (0.840–1.000, 95% CI, $p < 0.001$) (Fig. 3). The sensitivity, specificity and accuracy values of the model in detecting patients with GG > 3 were calculated as 85.7%, 85% and 85.4%. The formula of the model was given in Table 4.

Discussion

The results of our study show that; model performance generated from the late PSMA PET radiomic data is more successful than the early PET model. The late model's AUC, sensitivity and accuracy values (0.924, 85.7%, 85.4%) were obtained at higher values than the early model (0.902, 76.2%, 78.1%). This shows us that late imaging may contribute more than early imaging in PSMA PET radiomic studies. To our knowledge, these results are reported for the first time in the literature with the current study.

With the development of radiomic analyses, it is expected to take its place in clinical use. There are a limited number of studies evaluating 68Ga-PSMA PET/CT radiomics in the literature. In a study with 68Ga-PSMA PET/CT radiomics conducted by Zamboglou et al., 20 patients who underwent radical prostatectomy followed by staging 68Ga-PSMA-11 PET/CT were prospectively analyzed; gross tumor volume (GTV-Exp) was obtained semi-automatically using 0–5 SUV window levels and GTV-40% by applying 40% threshold of intraprostatic SUVmax [14]. QSZHGE showed better performance in distinguishing Gleason Score (GS) 7 and ≥ 8 ($p < 0.05$). However, for GTV-40%, no feature was found to be strongly associated with GS. In addition to PSMA PET radiomic studies so far, the results of our study prove that late PET radiomic features will increase the success of the model. Our results suggest that radiomic analyses of PSMA expression in the prostate gland on diagnostic 68Ga-PSMA PET/CT images may help clinicians to predict non-invasive GG groups and to determine risk groups better.

The features that we included in the models obtained were GLRLM_RLNU and SHAPE_compacity. GLRLM_RLNU defines the non-uniformity of run lengths throughout the image. A lower value of RLNU indicates more homogeneity among run lengths in the image while high values show the heterogeneity. The SHAPE_compacity feature also shows how compact the area of interest is. Both the GLRLM_RLNU and SHAPE_compacity features

were higher in patients with GG > 3, indicating greater heterogeneity of high-grade tumors.

Since it is the lowest SUV used in automatic programs in the literature, we have determined a cutoff of 2.5 SUVmax [22]. We also tried to make a more standard evaluation using the same cutoff for both early and late images. Zamboglou et al. found no feature strongly associated with GS for GTV-40% [14]. We also did not use a special percent threshold value and were able to obtain successful results in our study.

Our results showed that Dmax was higher in patients with high GG. In other words, it has been quantitatively shown that metastatic spread is higher in tumors with high aggressiveness. Dmax was correlated with both tumor volumetric parameters in the whole body and PSA, the biochemical indicator of PCa. We were also able to show that the tumor spread may be different according to the GG group in patients with metastatic tumors and therefore included in high-risk patients. The prognostic significance of this newly defined feature in patients with PCa needs to be further investigated.

Moreover, our results showed that volumetric parameters were more successful than SUV parameters in distinguishing GG groups, and these results are in line with the literature [24].

The retrospective nature of the study was one of the limitations of this study. And also the histopathological correlation was not technically and ethically possible from all foci with metastasis. Second- or higher-order features of tumors with a volume of interest less than 64 voxels cannot be obtained in the LIFEx software, because second-order or higher-order features are usually obtained by quantizing adjacent pixels to a separate set of values [19]. Therefore, patients with more than 64 voxels were included in our study. Also, previous studies have shown that conditions such as image acquisition, reconstruction, pre-processing and segmentation could affect radiomic features [25–27]. So, texture analyses studies may need standardization of imaging techniques and derivation of features.

In conclusion, without using invasive methods, 68Ga-PSMA PET/CT images will be able to detect primary tumor and metastasis of PCa, as well as assess heterogeneity and aggressiveness of primary tumor and predict GG groups. All these parameters may help clinicians for personal treatment planning and early decision making. Late imaging increases the performance of the obtained radiomic model. These findings should be supported by large patient groups in prospective studies.

Funding The authors received no financial support for the research and/or authorship of this article.

Declarations

Conflict of interest The authors declared no conflicts of interest with respect to the authorship and/or publication of this article.

References

1. Afshar-Oromieh A, Malcher A, Eder M, Eisenhut M, Linhart HG, Hadaschik BA, et al. PET imaging with a [68Ga]gallium-labelled PSMA ligand for the diagnosis of prostate cancer: biodistribution in humans and first evaluation of tumour lesions. Eur J Nucl Med Mol Imaging. 2013;40(4):486–95.
2. Eiber M, Maurer T, Souvatzoglou M, Beer AJ, Ruffani A, Haller B, et al. Evaluation of hybrid 68Ga-PSMA Ligand PET/CT in 248 patients with biochemical recurrence after radical prostatectomy. J Nucl Med. 2015;56(5):668–74.
3. Perera M, Papa N, Christidis D, Wetherell D, Hofman MS, Murphy DG, et al. Sensitivity, specificity, and predictors of positive (68)Ga-prostate-specific membrane antigen positron emission tomography in advanced prostate cancer: a systematic review and meta-analyses. Eur Urol. 2016;70:926–37.
4. Han S, Woo S, Kim YJ, Suh CH. Impact of (68)Ga-PSMA PET on the management of patients with prostate cancer: a systematic review and meta-analyses. Eur Urol. 2018;74(2):179–90.
5. Schmidkonz C, Cordes M, Schmidt D, Bauerle T, Goetz TI, Beck M, et al. (68)Ga-PSMA-11 PET/CT-derived metabolic parameters for determination of whole-body tumor burden and treatment response in prostate cancer. Eur J Nucl Med Mol Imaging. 2018;45(11):1862–72.
6. Schmuck S, von Klot CA, Henkenberens C, Sohns JM, Christiansen H, Wester HJ, et al. Initial experience with volumetric 68Ga-PSMA I&T PET/CT for assessment of whole-body tumor burden as a quantitative imaging biomarker in patients with prostate cancer. J Nucl Med. 2017;58(12):1962–8.
7. Acar E, Özdoğan Ö, Aksu A, Derebek E, Bekiş R, Çapa KG. The use of molecular volumetric parameters for the evaluation of Lu-177 PSMA I&T therapy response and survival. Ann Nucl Med. 2019;33(9):681–8.
8. Cottereau AS, Nioche C, Dirand AS, Clerc J, Morschhauser F, Casasnovas O, et al. 18F-FDG PET dissemination features in diffuse large B-Cell lymphoma are predictive of outcome. J Nucl Med. 2020;61(1):40–5.
9. Gillies RJ, Kinahan PE, Hricak H. Radiomics: images are more than pictures. They are data. Radiology. 2016;278(2):563–77.
10. Hyun SH, Ahn MS, Koh YW, Lee SJ. A machine-learning approach using PET-based radiomics to predict the histological subtypes of lung cancer. Clin Nucl Med. 2019;44(12):956–60.
11. Li Y, Zhang Y, Fang Q, Zhang X, Hou P, Wu H, et al. Radiomics analyses of [18F]FDG PET/CT for microvascular invasion and prognosis prediction in very-early- and early-stage hepatocellular carcinoma. Eur J Nucl Med Mol Imaging. 2021;48(8):2599–614.
12. Polverari G, Ceci F, Bertaglia V, Reale ML, Rampado O, Gallio E, et al. 18F-FDG pet parameters and radiomics features analyses in advanced Nsclc treated with immunotherapy as predictors of therapy response and survival. Cancers (Basel). 2020;12(5):1163.
13. Giannini V, Mazzetti S, Bertotto I, Chiarenza C, Cauda S, Delmastro E, et al. Predicting locally advanced rectal cancer response to neoadjuvant therapy with 18F-FDG PET and MRI radiomics features. Eur J Nucl Med Mol Imaging. 2019;46(4):878–88.
14. Zamboglou C, Carles M, Fechter T, Kiefer S, Reichel K, Fass-bender TF, et al. Radiomic features from PSMA PET for non-invasive intraprostatic tumor discrimination and characterization in patients with intermediate- and high-risk prostate

cancer—a comparison study with histology reference. Theranostics. 2019;9(9):2595–605.
15. Zamboglou C, Bettermann AS, Gratzke C, Mix M, Ruf J, Kiefer S, et al. Uncovering the invisible-prevalence, characteristics, and radiomics feature-based detection of visually undetectable intraprostatic tumor lesions in 68GaPSMA-11 PET images of patients with primary prostate cancer. Eur J Nucl Med Mol Imaging. 2021;48(6):1987–97.
16. Papp L, Spielvogel CP, Grubmüller B, Grahovac M, Krajnc D, Ecsedi B, et al. Supervised machine learning enables non-invasive lesion characterization in primary prostate cancer with [68Ga]Ga-PSMA-11 PET/MRI. Eur J Nucl Med Mol Imaging. 2021;48(6):1795–805.
17. Alberts I, Sachpekidis C, Dijkstra L, Prenosil G, Gourni E, Boxler S, et al. The role of additional late PSMA-ligand PET/CT in the differentiation between lymph node metastases and ganglia. Eur J Nucl Med Mol Imaging. 2020;47:642–51. https://doi.org/10.1007/s00259-019-04552-9.
18. Schmuck S, Mamach M, Wilke F, von Klot CA, Henkenberens C, Thackeray JT, Sohns JM, et al. Multiple time-point 68Ga-PSMA I&T PET/CT for characterization of primary prostate cancer: value of early dynamic and delayed imaging. Clin Nucl Med. 2017;42:286–93.
19. Nioche C, Orlhac F, Soussan M, Boughdad S, Alberini J, Buvat I. A software for characterizing intra-tumor heterogeneity in multimodality imaging and establishing reference charts. Eur J Nucl Med Mol Imaging. 2016;43:S156–7.
20. Epstein JI, Egevad L, Amin MB, Delahunt B, Srigley JR, Humphrey PA. The 2014 international society of urological pathology (ISUP) consensus conference on Gleason grading of prostatic carcinoma. Am J Surg Pathol. 2016;40(2):244–52.
21. Rowe SP, Pienta KJ, Pomper MG, Gorin MA. PSMA-RADS version 1.0: a step towards standardizing the interpretation and reporting of PSMA-targeted PET imaging studies. Eur Urol. 2018;73(4):485–7.
22. Hammes J, Täger P, Drzezga A. EBONI: a tool for automated quantification of bone metastasis load in PSMA PET/CT. J Nucl Med. 2018;59(7):1070–5. https://doi.org/10.2967/jnumed.117.203265 (**Epub 2017 Dec 14**).
23. Chan YH. Biostatistics 104: correlational analyses. Singap Med J. 2003;44:614–9.
24. Aksu A, Karahan Şen NP, Tuna EB, Aslan G, Çapa KG. Evaluation of 68Ga-PSMA PET/CT with volumetric parameters for staging of prostate cancer patients. Nucl Med Commun. 2021;42(5):503–9.
25. Shiri I, Rahmim A, Ghaffarian P, Geramifar P, Abdollahi H, Bitarafan-Rajabi A. The impact of image reconstruction settings on 18F-FDG PET radiomic features: multi-scanner phantom and patient studies. Eur Radiol. 2017;27(11):4498–509.
26. Leijenaar RT, Nalbantov G, Carvalho S, van Elmpt WJ, Troost EG, Boellaard R, et al. The effect of SUV discretization in quantitative FDG-PET radiomics: the need for standardized methodology in tumor texture analyses. Sci Rep. 2015;5(5):11075.
27. van Velden FH, Kramer GM, Frings V, Nissen IA, Mulder ER, de Langen A, et al. Repeatability of radiomic features in non-small-cell lung cancer [(18)F]FDG-PET/CT studies: ımpact of reconstruction and delineation. Mol Imaging Biol. 2016;18(5):788–95.